

## Central Lancashire Online Knowledge (CLoK)

Title	Smoke toxicity of fire protecting timber treatments
Type	Article
URL	<a href="https://clock.uclan.ac.uk/49162/">https://clock.uclan.ac.uk/49162/</a>
DOI	##doi##
Date	2023
Citation	Hansen-Bruhn, Iben and Hull, T Richard orcid iconORCID: 0000-0002-7970-4208 (2023) Smoke toxicity of fire protecting timber treatments. Fire Safety Journal, 141 . p. 103977. ISSN 0379-7112
Creators	Hansen-Bruhn, Iben and Hull, T Richard

It is advisable to refer to the publisher's version if you intend to cite from the work. ##doi##

For information about Research at UCLan please go to <http://www.uclan.ac.uk/research/>

All outputs in CLoK are protected by Intellectual Property Rights law, including Copyright law. Copyright, IPR and Moral Rights for the works on this site are retained by the individual authors and/or other copyright owners. Terms and conditions for use of this material are defined in the <http://clock.uclan.ac.uk/policies/>



# Smoke toxicity of fire protecting timber treatments

Iben Hansen-Bruhn<sup>a,b,c</sup>, T. Richard Hull<sup>a,\*</sup>

<sup>a</sup> Centre for Fire and Hazard Science, University of Central Lancashire, Preston, PR1 2HE, UK

<sup>b</sup> Plastic and Polymer Engineering, Department of Biological and Chemical Engineering, Aarhus University, Aabogade 40, 8200, Aarhus N, Denmark

<sup>c</sup> Teknos Fire Retardant Technology, R&D, Teknos A/S, Industrivej 19, DK-6580, Vandrup, Denmark

## ARTICLE INFO

### Keywords:

Fire chemistry  
Risk assessment  
Smoke  
Toxicity  
Hazard evaluation  
Protection of wood

## ABSTRACT

Most fire deaths arise from inhalation of toxic gases. The fire toxicity of untreated plywood, pressure impregnated plywood and surface coated plywood was investigated under a range of fire conditions. Using the steady state tube furnace individual fire stages were replicated, fire effluent sampled, and toxic product yield determined by high performance ion chromatography and spectrophotometry. Despite different phosphorus loadings, both treatments hindered developing fires with less than 50% mass loss during non-flaming oxidative pyrolysis and did not readily undergo steady flaming. During under-ventilated flaming, all samples produced hydrogen cyanide (HCN), and both fire protecting treatments produced phosphoric acid (H<sub>3</sub>PO<sub>4</sub>). Assessment of smoke toxicity as fractional effective dose for incapacitation was based on asphyxiants carbon monoxide (CO) and hydrogen cyanide (HCN). This work demonstrates that due to emission of large amounts of CO, the predicted smoke toxicity of impregnated timber is significantly higher than coated timbers when a growing fire reaches the under-ventilated stage. The results have clear implications for those selecting products to ensure fire safety in enclosures such as buildings.

## 1. Introduction

Timber is enjoying a renaissance as the sustainable alternative to the more climate harming construction materials such as concrete, brick and steel [1]. Timber has some ability to resist fire, through the sacrificial burning of a few outer millimetres to form a carbonaceous char, which slows the rate of fire penetration to around 0.6 mm min<sup>-1</sup> [2]. Thus, large structural elements, such as timber beams, can be effective in preventing collapse of a burning building, during and after evacuation. The aesthetic properties of timber, and perhaps its green credentials, have also encouraged its wider use where smaller non-structural sections are required. However, as an inherently combustible material, it presents a different set of challenges in fire safety [3–5].

Fire retardants are typically either coated onto the surface of the wood or impregnated into the wood structure using a vacuum-pressure technique [6,7].

**Surface Treatment:** To apply a fire protecting surface coating to wood, it is typically painted, sprayed, or dipped into a treatment suspension. Superficial treatments, such as coatings, are easily applied, and a comparatively small amount of the suspension is required for fire protection. However, there may be subsequent re-application

requirements and the possibility of surface damage [8]. The fire retardant coats the wood to provide a fire protective barrier, inhibiting heat transfer and preventing the escape of flammable vapours and access of oxygen. Typical barrier coatings have an intumescent formulation which swells on heating to create a protective carbonaceous foam [9].

**Pressure Impregnation:** Wood has a spongy structure with cell cavities and cell walls penetrable to impregnation [10]. Fire retardants coat the cells walls to protect the structure. First, air is evacuated from the cavities to allow access by the fire retardant treatment solution, which is then forced deep into the wood by high pressure. However, impregnated surfaces are difficult to varnish, and outdoor weathering may result in subsequent leaching [11,12]. The parameters can be adjusted to tailor the treatment, dependent on the level of protection and the depth profile of fire retardant required. In general, impregnation inhibits pyrolysis of wood, and increases char and water formation [13].

Most fire deaths and most fire injuries result from inhalation of toxic fire effluents [14]. Smoke toxicity is recognised as a major factor in the assessment of fire hazard. Replacement of prescriptive standards by performance-based fire codes requires assessment by fire safety engineers, which includes prediction of the smoke toxicity distribution within a building. This depends on two parameters:

\* Corresponding author.

E-mail addresses: [iben.hansenbruhn@teknos.com](mailto:iben.hansenbruhn@teknos.com) (I. Hansen-Bruhn), [TRHull@uclan.ac.uk](mailto:TRHull@uclan.ac.uk) (T.R. Hull).

<https://doi.org/10.1016/j.firesaf.2023.103977>

Received 9 June 2023; Received in revised form 24 August 2023; Accepted 14 September 2023

Available online 14 September 2023

0379-7112/© 2023 The Authors. Published by Elsevier Ltd. This is an open access article under the CC BY license (<http://creativecommons.org/licenses/by/4.0/>).

- Time-concentration profiles for major products. These depend on the fire growth curve and the yields of toxic products.
- Toxicity of the products, based on estimates of doses likely to impair escape efficiency, cause incapacitation, or death.

Toxic product yields depend on the material composition, and the fire conditions [15]. The burning of an organic material, such as timber, is a complex process where non-volatile components degrade into volatile breakdown products, which react with oxygen, producing a cocktail of products. These range from the relatively harmless carbon dioxide (CO<sub>2</sub>) and water to products of incomplete combustion, including carbon monoxide (CO), hydrogen cyanide (HCN), nitrogen oxides (NO<sub>x</sub>) and organoairritants. Depending on the presence of other chemical elements, halogen acids, phosphorus and sulphur compounds may also be formed.

The greatest difference in fire conditions on smoke toxicity arises between flaming and non-flaming combustion. Non-flaming typically produces a small volume of highly toxic smoke. For flaming combustion, the fuel-to-air ratio has the largest effect on the toxic product yield. As a fire in an enclosure develops, the temperature increases and oxygen concentration decreases. Research, reviewed by Pitts [16], predicting the CO evolution from simple hydrocarbon flames, has shown the importance of the fuel-to-air equivalence ratio,  $\phi$ , in correlating the CO yield to the ventilation condition during flaming.

$\phi = \frac{\text{actual fuel to air ratio}}{\text{stoichiometric fuel to air ratio}}$		Typical CO yield g/g
$\phi \sim 0.7$	fuel lean flames	0.01
$\phi = 1.0$	stoichiometric flames	0.05
$\phi \sim 1.5$	fuel rich flames	0.20

For many materials containing carbon, hydrogen, and oxygen, the CO yield increases rapidly with increase in  $\phi$ , and almost independent of polymer [17]. In addition, a close correlation between CO formation and HCN formation has been established in full-scale fire studies [18,19], as the formation of both species appears to be favourable in under-ventilated conditions [20].

In terms of contribution to smoke toxicity [19], fire progress through stages from non-flaming to well-ventilated flaming, and finally to under-ventilated flaming. These have been classified by ISO 19706 [21] (Table 1) in terms of heat flux, temperature, oxygen concentration (to the fire, and in the fire effluent), and CO/CO<sub>2</sub> ratio, equivalence ratio  $\phi$ , and combustion efficiency (%-conversion of fuel to fully oxygenated products, such as CO<sub>2</sub> and water). While some fires may be represented by a single stage, most will grow through several stages. On some occasions, smouldering (oxidative pyrolysis) can be important, such as in timber, especially after a major fire, but the rate of reaction, and hence the amount of toxic species generated, will be small. Similarly, well-ventilated fires are generally small, so extinguishment or escape is still feasible, and any movement of fire effluent will be between head

height and the ceiling. However, as they grow, fires become ventilation-controlled, and fires in enclosures can change rapidly from well-ventilated to under-ventilated. Under-ventilated fires are large, relative to the size of the enclosure, and therefore produce large quantities of effluent, endangering occupants over a much greater volume of the enclosure than well-ventilated fires. While well-ventilated fire scenarios are correctly used for assessment of flammability, fire toxicity is assessed to prevent loss of life or injury, where the important fire stages are under-ventilated (Table 1). CO/CO<sub>2</sub> ratios can only be used to characterise fire stages for burning materials that do not contain chlorine or bromine, since they significantly increase the CO yield in well-ventilated fires.

Smoke not only reduces visibility, hindering escape, but its gases have irritating and lethal toxic effects. Primary products of wood combustion include CO, CO<sub>2</sub> and water [22]. However, hydrogen cyanide and hydrogen halides can be released if heteroelements such as nitrogen or halogens are present. Fire retardants often contain such heteroelements, which can increase the yield of smoke and its toxic components, but by slowing the rate of burning, also may cause a net reduction in smoke and toxic gas production rates.

CO is one of the most toxicologically significant components in fire gases, preventing oxygen transport by the formation of carboxyhaemoglobin. HCN is also important because it prevents uptake of oxygen by the cells. The presence of CO<sub>2</sub> in blood, which stimulates hyperventilation, increases the respiration rate and hence the hazard from the toxic components of the fire gas. Oxygen depletion also deprives the body of oxygen (hypoxia) with fatal consequences at concentrations below 13%. To predict the effects of the toxicants on humans the measured data must be combined using established models of toxicity. Incapacitation, or “the inability to effect one’s own escape” is the critical point leading to fatality, in the absence of rescue personnel. Incapacitation resulting from the asphyxiant gases in fire effluents (HCN and CO) can be predicted using the equations presented in ISO 13571 [23].

Toxic effects of fire effluent can be expressed as a Fractional Effective Dose (FED), based on the chemical composition of the effluent. When the FED is equal to one, 50% of a healthy, adult exposed population are predicted to succumb. The end-point could be incapacitation or death. In both cases carbon dioxide (CO<sub>2</sub>) increases respiration rate and so a multiplication factor for CO<sub>2</sub>-driven hyperventilation,  $\nu_{CO_2}$ , is included in the calculation (Eq. (2)). ISO 13571 [23] stipulates the use of Eq. (1) for estimation of incapacitation by the asphyxiant gases carbon monoxide (CO) and hydrogen cyanide (HCN):

$$FED = \left\{ \sum_{t_1}^{t_2} \frac{[CO]}{35000} \Delta t + \sum_{t_1}^{t_2} \frac{[HCN]^{2.36}}{1.2 \times 10^6} \Delta t \right\} \times \nu_{CO_2} \tag{1}$$

$$\nu_{CO_2} = \exp\left(\frac{[CO_2]}{50000}\right) \tag{2}$$

Gas concentrations in [ ] are expressed in  $\mu\text{L L}^{-1}$  or ppm; time ( $t$ ) is in minutes.

**Table 1**  
ISO classification of fire stages given in ISO 19706 (adapted) [21].

Fire Stage	Heat /kW m <sup>-2</sup>	Max Temp/°C		Oxygen/%		$\phi$	CO/CO <sub>2</sub>	Combustion Efficiency /%
		Fuel	Smoke	In	Out			
<b>Stage 1: Non-flaming</b>								
1a. Self- sustained smouldering	NA	450–800	25–85	20	0–20	–	0.1–1	50–90
1b. Oxidative, external radiation	–	300–600		20	20	–		
1c. Anaerobic external radiation	–	100–500		0	0	–		
<b>Stage 2: Well ventilated flaming</b>								
2. Well vent. Flaming	0–60	350–650	50–500	~20	0–20	<0.8	<0.05	>95
<b>Stage 3: Under ventilated flaming</b>								
3a. Low vent. room fire	0–30	300–600	50–500	15–20	5–10	>1.2	0.2–0.4	70–80
3b. Post flashover	50–150	350–650	>600	<15	<5	>1.2	0.1–0.4	70–90

It is important to recognise that hazard prediction describes an unacceptable outcome of incapacitation or lethality. In any hazard or risk assessment, a factor of 0.3 is applied for a healthy adult population to ensure that around 90% of the trapped fire victims do not suffer the outcomes above, and another factor of 0.3 is applied to that figure if typical human populations, such as office workers, are considered, in order to account for individuals of greater susceptibility. Thus, a value of  $FED = 0.1$  for effluent flowing into an apartment could be considered the maximum permissible hazard.

The steady state tube furnace, ISO/TS 19700 [24] has proved suitable for investigating the effect of fire protecting treatments and fire conditions on the toxic product yields and the predicted combustion toxicity [25,26]. This is one of the only techniques capable of replicating all fire conditions including under-ventilated combustion [27]. The apparatus may be set up to burn material either without flaming or, for flammable samples, at a particular equivalence ratio, from well-ventilated flaming to the more toxic under-ventilated flaming. It is designed to force a fixed rate of burning by feeding a long, linear sample into a furnace of increasing heat flux at a fixed feed rate. Initially, the sample will ignite when the critical heat flux for spontaneous ignition is reached, but the flame will then move back along the sample to the point where the critical heat flux for piloted ignition is located in the furnace. At this point, steady flaming will continue as the sample continues to be fed into the furnace. The fuel-to-air ratio profoundly affects the results, but within the sample mass feed rate range of  $0.5\text{--}2\text{ g min}^{-1}$ , consistent toxic product yields are obtained across the range of fuel-to-air ratios. This enables it to provide reliable data on the toxic product yields as a function of equivalence ratio. Unlike a “flammability test” [28] where a material’s chemistry dictates the rate of burning, in the steady state tube furnace all flammable materials are burned at a fixed rate.

This study aims to assess the smoke toxicity under the range of fire conditions of three materials: untreated plywood; plywood treated by surface coating with an ammonium polyphosphate (APP) based intumescent formulation; and plywood treated by vacuum-pressure impregnation with an ammonium phosphate (MAP) treatment. Environmentally-greener boric acid-free impregnation treatment, and melamine-free waterborne coating treatments were investigated to inform the choices of architects and engineers.

## 2. Material and methods

Three samples prepared from two boards ( $12\text{ mm} \times 1230\text{ mm} \times 1500\text{ mm}$ ), were tested in this study. Plywood boards, specified as pine, were acquired from a commercial supplier of impregnated boards in an untreated (*Pine*) and pressure impregnation treated version (*FRP*) (boric acid free, phosphorus based, Euroclass B-s1, d0). The third sample (*FRC*) was prepared in our laboratory by application of a water-based melamine-free fire retardant intumescent coating (Teknosafe Flame Guard, Teknos, DK) on the untreated board, as specified in the technical data sheet, to obtain Euroclass B-s1, d0.

### 2.1. Sample preparation

With a band saw, 10 mm strips ( $1230\text{ mm} \times 12\text{ mm}$ ) were cut, rotated by  $90^\circ$ , then cut along the length axis with the blade parallel to the plies of the board giving a final thickness of 3–4 mm and with approximately two plywood layers in each sample. Final dimensions were  $800\text{ mm} \times 10\text{ mm} \times (3\text{--}4)\text{ mm}$ . This was necessary to obtain representative, linearly uniform samples of appropriate mass for testing. Some of the 10 mm *Pine* strips were spray-coated with about  $400\text{ }\mu\text{m}$  (when wet) coating, dried in air at  $20 \pm 3\text{ }^\circ\text{C}$  and RH around 50%, and then cut to final dimensions  $800\text{ mm} \times 10\text{ mm} \times (8\text{--}9)\text{ mm}$  as described above with coating on three of four sides. Mass and dimensions of each sample was noted before testing, to obtain sample density.

### 2.2. Sample characterisation

Samples were characterized by scanning electron microscopy, SEM-EDAX (Quattro ESEM, ETD detector, Thermo Scientific, USA), and attenuated total reflectance Fourier transform infrared spectrophotometry, ATR-FTIR (iS50 fitted with iD5, ZnSe crystal, Thermo Scientific, USA). *Pine* was additionally characterised with elemental analysis ( $n = 4$ ) using CHNS (Flash 2000 Organic Elemental Analyser, Thermo Scientific, USA).

### 2.3. Steady state tube furnace (SSTF)

The steady state tube furnace (SSTF) apparatus is shown in Fig. 1. Samples were fed into the furnace in an 800 mm quartz boat to give a mass feed rate of approximately  $1\text{ g min}^{-1}$ . By varying the primary air flow rate, fire conditions were created at different equivalence ratios. Following the guidance in the standard, the furnace temperature was increased in an attempt to obtain steady flaming. The combustion products flowed from the tube furnace into the mixing chamber, where they were diluted to a constant volume of  $50\text{ L min}^{-1}$ . Samples of the effluent were filtered, and analysed in real time, or passed directly into bubblers trapping individual toxic components for subsequent analysis. Oxygen depletion and yields of carbon dioxide, carbon monoxide and smoke were determined for each fire condition, as previously reported [29,30]. Gas samples were collected by drawing a metered volume of fire gas effluent through bubblers and determined using high performance ion chromatography (HPIC) and spectrophotometric techniques according to ISO 19701 [31].

*Pine*, *FRP*, and *FRC* were tested in the steady state tube furnace (SSTF) in accordance with ISO/TS 19700 with total air flow of  $50\text{ L min}^{-1}$  and sample mass feed rate of  $1.0 \pm 0.1\text{ g min}^{-1}$  in all runs. With variation of experimental parameters, such as primary air flow (from  $2\text{ L min}^{-1}$  to  $10\text{ L min}^{-1}$ ), specimen boat speed ( $20\text{--}50\text{ mm min}^{-1}$ ), and furnace temperature ( $350\text{ }^\circ\text{C}\text{--}875\text{ }^\circ\text{C}$ ), each sample was tested in fire stage 1b (oxidative pyrolysis from externally applied radiation), 2 (well-ventilated flaming), 3a (under-ventilated flaming in a small, localised area/poorly ventilated compartment), and where possible, 3b (post-flashover fire). For stage 1b and 2, samples were tested in triplicate with fire effluent gas sampling for off-line quantification in two of three runs, whereas for stage 3a and 3b single experiments were conducted. In contrast to test runs with *Pine*, where steady flaming occurred at  $650\text{ }^\circ\text{C}$ , the furnace temperature needed to be increased to  $875\text{ }^\circ\text{C}$  for *FRP* and *FRC* to obtain steady flaming. Additionally, for each sample type, a test series with variation of primary air flow under constant furnace temperature (ensuring flaming combustion) was set up to obtain test runs with different equivalence ratios,  $\varphi$ , ranging from well-ventilated to under-ventilated flaming. The total number of steady state experiments for each sample was: *Pine* (21), *FRP* (16), *FRC* (17); with 6, 5, and 5 sample-fire condition combinations respectively, with fire effluent sampling for off-line quantification as described in section 2.3.1. Data were collected over the steady state burning period (minimum 5 min) to obtain an average yield. During this time samples were also collected in bubbler solutions (for HPIC analysis of  $\text{CN}^-$ ,  $\text{F}^-$ ,  $\text{Cl}^-$ ,  $\text{Br}^-$ ,  $\text{NO}_3^-$ ,  $\text{NO}_2^-$ ,  $\text{SO}_4^{2-}$ , and  $\text{PO}_4^{3-}$  and spectrophotometric analysis of  $\text{CN}^-$ ).

#### 2.3.1. Fire effluent sampling and analysis

After dilution with secondary air, fire effluent was sampled from the mixing chamber at  $1.0\text{ L min}^{-1}$  through a primary line to a set of gas analysers. Another stream was passed at  $1.0\text{ L min}^{-1}$  via a secondary line into an oxidiser furnace ( $900\text{ }^\circ\text{C}$ ) and to a second set of gas analysers. To avoid blockage of pumps and analysers, the fire gas was passed through soot traps (glass columns lightly packed with glass wool), drying tubes (silica/drierite packed between glass wool plugs), and finally a HEPA filter to ensure the absence of particles. A third and fourth stream, sampled during steady state burning was passed through trains of Drechsel bottles with perforated bulbs into absorbing solutions.

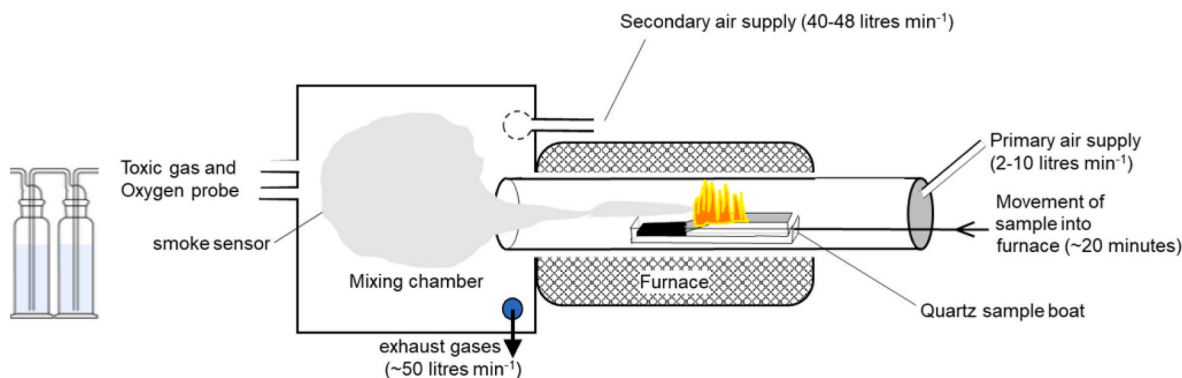


Fig. 1. The steady state tube furnace apparatus.

*In-line* continuous analysis to measure permanent combustion gases used a combination of non-dispersive infrared analysers (NDIR), electrochemical cells (EC) and paramagnetic oxygen analysers (PM). The sequence of analysers in the primary line are: NDIR CO<sub>2</sub> with 0–10% range (GasCard NG, Edinburgh Sensors Ltd, UK), EC CO with 0–4000 ppm range (CiTiceL, City Technology Ltd, UK), EC CO with 0–20000 ppm range (CiTiceL, City Technology Ltd, UK), and lastly PM O<sub>2</sub> (Paramagnetic analyser 570A, Servomex, UK). Before the PM O<sub>2</sub> analyser, the fire gas passed through an ascarite column (8–20 mesh, Sigma Aldrich, US) to remove CO<sub>2</sub> and water. Analysers for the secondary line are: EC O<sub>2</sub> (Andros, Lumasence Technologies, DE) and NDIR CO<sub>2</sub> with 0–10% range (GasCard NG, Edinburgh Sensors Ltd, UK). The voltage output from each analyser was connected to an analogue-to-digital data acquisition unit (Personal Daq/50, IO Tech, UK) and via USB cable to a PC. Calibration of the gas analysers were performed with gas bags (Tedlar bags, 24" x 24.25", Restek, UK) filled with analytical grade gas (N<sub>2</sub>, CO<sub>2</sub>/CO mixtures of 4%/6000 ppm and 8%/2000 ppm). Attenuation of a laser beam by smoke (3 mW 635 nm CW, 213–3584, RS Components Ltd, UK) was measured with a photodiode (BPW21R, RS Components Ltd, UK) throughout each run and pre-calibrated with filters of optical density 0.3 and 0.8.

For *off-line* quantification of other species two separate ports were connected to Dreschel bottles (bubblers) containing either deionised water or 0.1 M NaOH: each 150 mL bubbler contained 75 mL of absorbing solution. Pumps were turned on during the steady state combustion period, and fire effluent was sampled for 5 min at 1.0 L min<sup>-1</sup> (SMC PFM710, RS Components, UK). Fire effluent solutions were stored in airtight polypropylene bottles in a dark cupboard at room temperature for further testing (details in section 2.4 and 2.5).

#### 2.4. Cyanide quantification with UV-vis spectrophotometry (UV-vis)

Bubbler-sampled fire effluent trapped in the NaOH absorbing solution was analysed ( $n = 4$ ) using the method outlined in ISO 19701 [31] and described in detail elsewhere [32]. All chemicals were analytical grade (Sigma Aldrich) if not otherwise specified.

As reagent A, 0.1 g chloramine-T was dissolved in 100 mL distilled water. Reagent B was prepared in two steps: 0.75 g 3-methyl-1-phenyl-2-pyrazoline-5-one was dissolved in 50 mL dimethyl formamide (DMF) mixed with (3.75 g isonicotinic acid in 50 mL 1 M NaOH adjusted to pH = 7.0 by 1 M HCl) and made up to 250 mL with distilled water. Further, a phosphate buffer solution was prepared (pH = 7.2). Cyanide standard solutions were prepared from a stock solution (0.3225 g KCN, Sigma Aldrich 97% up to 250 mL with 0.1 M NaOH) and diluted accordingly to make 0.3, 0.8, 2.0, 5.0 and 8.0 mg L<sup>-1</sup> standards. The cyanide standards were stored in a refrigerator until required.

To a test tube, the following were added sequentially: 1.00 mL cyanide test solution, 9.00 mL distilled water, 4.50 mL phosphate buffer, 2.0 mL reagent A, and after 5 min, 4.5 mL reagent B. After a further 30

min, the absorbance was measured at 638 nm with two ultraviolet-visible (UV-vis) spectrophotometers (WPA lightwave II, Biochrom Ltd., UK), in either 10 mm and 40 mm cuvettes. 0.1 mol L<sup>-1</sup> NaOH was used instead of the 1 mL cyanide test solution and treated as above, as a blank.

#### 2.5. High performance ion chromatography (HPIC)

Fire effluents solution were analysed with high performance ion chromatography, HPIC, to give their concentrations as electrical conductivity/current versus retention time data (Dionex, Thermo Scientific equipped with AS-AP autosampler and two units: Aquion-Anion unit with AERS 500 Carbonate Suppressor (2 mm), and Integriion unit equipped an ICS-6000/4000 ED electrochemical detector cell (pulsed amperometric detection, pH-Ag/AgCl reference electrode and Ag working electrode) and eluent degas system). All solutions were prepared with deionised water, and all chemicals were analytical grade (Sigma Aldrich) if not otherwise specified.

The Aquion-Anion unit was used for quantification of the following ions: F<sup>-</sup>, Cl<sup>-</sup>, Br<sup>-</sup>, NO<sub>3</sub><sup>-</sup>, NO<sub>2</sub><sup>-</sup>, SO<sub>4</sub><sup>2-</sup>, and PO<sub>4</sub><sup>3-</sup> in fire effluent bubbler solutions. Using a 2 mL syringe, fire effluent solution was transferred through a syringe filter (0.22 μm polyether sulphone, Choice 25 mm, Thermo Scientific) to a 1.5 mL polypropylene vial with cap and septa. Test solutions and ion calibration standards (0.25, 0.50, 1.00, 2.50, 5.00, 10.00, 15.0, 30.0 mg L<sup>-1</sup> prepared from sodium salts) were measured twice with blanks (deionised water) between each set of measurements. Test solution (2.5 μL) was injected into the HPIC into an eluent flow of 0.3 mL min<sup>-1</sup>. The carbonate/bicarbonate eluant (4.5 mmol L<sup>-1</sup> Na<sub>2</sub>CO<sub>3</sub>/1.4 mmol L<sup>-1</sup> NaHCO<sub>3</sub>) took the analyte to a thermostatted (30 °C) precolumn (Dionex IonPac AG22, 50 mm × 4 mm, Thermo Scientific), and subsequently to an analytical column (Dionex IonPac AS22, alkanol quaternary ammonium resin, 250 mm × 4 mm, Thermo Scientific), prior to the quantification by the detector.

An Integriion unit was used for quantification of cyanide (CN<sup>-</sup>) in fire effluent captured in NaOH. If cyanide quantification, using the spectrophotometric technique described in section 2.5 showed concentrations exceeding 8.0 mg L<sup>-1</sup>, samples were diluted with 0.1 mol L<sup>-1</sup> NaOH to below the threshold. Calibration standards from section 2.4 were used. Analyte solutions (2.5 μL) were injected with a flow of 0.25 mL min<sup>-1</sup> acetate eluant (0.5 mol L<sup>-1</sup> Na<sub>2</sub>CO<sub>3</sub>/0.1 mol L<sup>-1</sup> NaOH/0.50 vol% ethylenediamine) to a thermostatted (30 °C) pre-column (Dionex IonPac AG7, 2 mm × 50 mm, Thermo Scientific), and subsequently to an analytical column (Dionex AS7, 2 mm × 50 mm, Thermo Scientific), prior to quantification by the detector.

For data capture and processing, Chromeleon Dionex software (v.7.2.10.23925, Thermo Scientific) was employed. After the baseline was established, the peaks identified were integrated, and from calibration curves, concentrations obtained for each ion present.

### 3. Results

Description and data for each sample are given in Table 2. The table summarizes information from supplier specifications, data sheets, and acquired analytical data (details are given in Supporting Information (SI), section S1 to S3).

Table 2 shows that based on SBI test results, both fire protecting treatments result in less smoke development (Euroclass s2 to s1) and reduction in contribution to fire from “medium” to “limited” (Euroclass D to B), compared to *Pine*. IR spectra together with elemental analysis of fire retardant coating reveal phosphorus bands from ammonium polyphosphate (APP) and traces of inorganics: all components expected were detected in intumescent fire retardant coating formulations. Functional groups ascribed to ammonium phosphate (MAP) were found in the IR spectrum for fire retarded pine, *FRP*. The *Pine* IR spectrum matches IR spectra reported in literature for wood [33,34]. The density difference between *Pine* and treated plywoods (*FRP* + 9.5%, *FRC* + 6.6%) is indicative of the dry fire retardant loading. The order of highest to lowest combustible content by mass is *FRC* (Coating without substrate) > *Pine* > *FRP*.

Toxicity data is usually presented in terms of yields of particular toxicants by mass of material from which the toxicants originated. The yields can be expressed as either mass-loss yields or mass-charge yields. In some cases, it is obvious which form should be used, for example if a 50 kg wall-lining is being installed in a room, and the assumption is that the flame could spread across it, then the mass-charge yield is appropriate. When the mass-loss varies significantly between samples, it is more appropriate to use the mass-loss yield to see how much toxicant derives from the same amount of volatile component. In the case of timber with different fire protecting treatments the situation is less clear cut. We have focused on the mass-loss yield, but since the mass losses are similar, the same trends would be observed for the mass-charge yield.

Fig. 2 summarizes the mass-loss yields of carbon monoxide (CO) obtained in the SSTF during steady state flaming combustion of *Pine* (650 °C), *FRP* (875 °C), and *FRC* (875 °C) with variation of equivalence ratio  $\phi$ . For both fire protected samples, a 5-min steady state flaming period was obtainable by increasing the furnace temperature to 875 °C, following the directions of ISO/TS 19700. For untreated *Pine* at least 12 min of steady state burning was obtainable (SI, section S4 and S5). Ignition times for all samples were found to be repeatable. Fig. 2 shows that the yields of CO for all samples remain very low during well-ventilated fires ( $\phi$  below 1) but increase with decreasing ventilation. However, for fires with an equivalence ratio above 1.5 combustion of *FRP* (red) generates significant higher amounts of CO compared to both *FRC* (blue) and *Pine* (black); around  $0.9 \text{ g g}^{-1}$  vs. less than  $0.3 \text{ g g}^{-1}$ .

Fig. 3 shows the smoke laser transmission during flaming combustion. Upon well-ventilated flaming with  $\phi$  below 1, *Pine* shows clean, orange flames with almost no smoke production (T% of 93), but during under-ventilated flaming, the transmittance fell to 33% (Fig. 3). In all

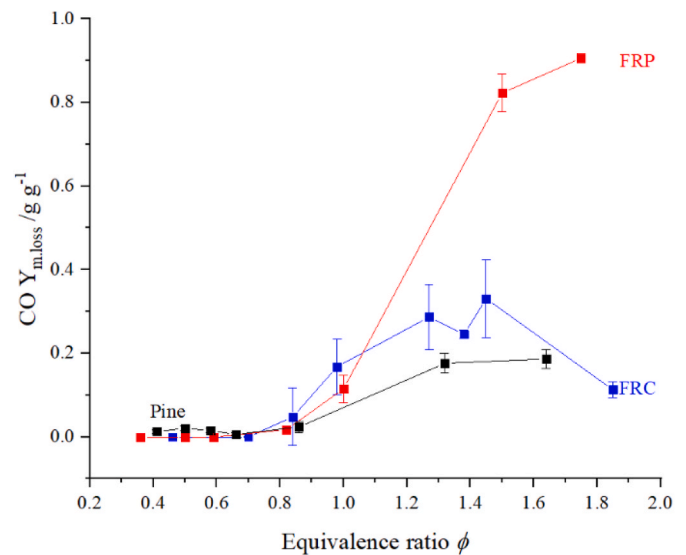


Fig. 2. Mass loss yields of CO during flaming combustion of *Pine* (black, 650 °C), *FRP* (red, 875 °C), and *FRC* (blue, 875 °C) with variation of equivalence ratios  $\phi$ . Lines are used to illustrate the trend. (For interpretation of the references to colour in this figure legend, the reader is referred to the Web version of this article.)

the SSTF fire tests *FRC* produced more smoke than *FRP*. An overview of mass-loss yield data from all fire stages tested is given in Table 3.

Beside CO and CO<sub>2</sub> production, Table 3 shows that all samples produced dense smoke during oxidative pyrolysis, fire stage 1b (transmittance less than 35%), but also left significant char residue. Both fire protective treatments showed reduced mass loss (45%–48%) compared to *Pine* (68%). During oxidative pyrolysis, *Pine* forms considerable amounts of oily, brown tar, which was not observed for *FRP* and *FRC*. In fire stage 3a, *FRP* stands out with less smoke production than both *Pine* and *FRC* (60%), but CO yield increased by a factor of 6–8. This was surprising, as CO and smoke levels usually accompany each other to indicate the extent of incomplete combustion. For all fire stages reported in Table 3, *FRC* produces more smoke, but less CO than *FRP*.

Table 4 summarizes the mass charge yields of asphyxiants (CO and HCN), and irritants (H<sub>3</sub>PO<sub>4</sub>) quantified in fire effluent sampled during steady state period of SSTF runs of *Pine*, *FRP*, and *FRC*. (Analytical results are found in SI, section S6, S7, and S8).

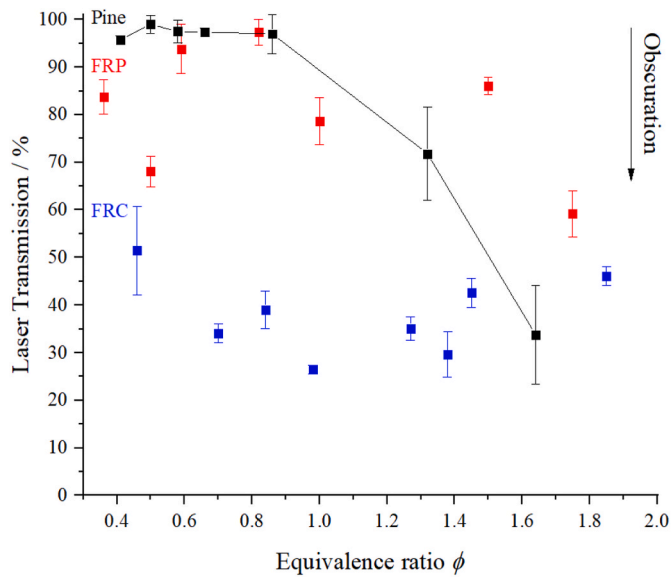
Table 4 shows that upon flaming, both types of fire protected timber produced H<sub>3</sub>PO<sub>4</sub> (detected as orthophosphate), and all samples produced HCN during under-ventilated flaming (fire stage 3a). Cyanide quantification is further validated by two different methods. For all fire effluent solutions, HPIC chromatograms did not show ions (above the detection limit) originating from fire gases HF, HBr, HCl, NO, NO<sub>2</sub>, or

Table 2

Sample data in overview.  $\rho$ : density. *DFT*: dry film thickness, averaged measurements from SEM images. Elemental composition from SEM-EDAX (For *Pine*, CHNS). Elemental composition of *FRC* is based on dried coating without substrate.

Sample	$\rho$ [kg m <sup>-3</sup> ]	Description	Elements [%]					ATR-FTIR
			C	H	O	N	P	
<i>Pine</i>	694	Non-treated 12 mm 9-layer pine plywood, D-s2, d0	48 (47)	-(6)	51 (45)	1.0 (1.7)	- <sup>a</sup>	Cellulose, hemicellulose, lignin bands
<i>FRC</i> Fire Retardant Coating	740	≈200 μm <i>DFT</i> on <i>Pine</i> substrate, B-s1, d0	40	- <sup>a</sup>	44	7.7	6.7	Ammonium poly-phosphate (APP) based coating
<i>FRP</i> Fire Retardant Pressure impregnated	760	12 mm 9-layer pine plywood, B-s1, d0	47	- <sup>a</sup>	48	3.2	1.8	Ammonium phosphate (MAP) based impregnation

<sup>a</sup> Below detection limit/not detectable by method.



**Fig. 3.** Smoke as laser transmittance versus equivalence ratio. A line was added to illustrate the trend for untreated plywood. The variation between tests, at different equivalence ratios, is attributed variation in size distribution of particulates.

**Table 3**  
Average mass loss yield data from SSTF for fire stages 1b, 2, 3a and 3b.

Fire stage	#	Test	$\phi$	Mass loss [%]	CO <sub>2</sub> Y <sub>m.loss</sub> [g g <sup>-1</sup> ]	CO Y <sub>m.loss</sub> [g g <sup>-1</sup> ]	Smoke [T%]
1b	3	P	NA <sup>b</sup>	68 (±5)	0.21 (±0.04)	0.08 (±0.01)	25 (±7)
	3	FRP	NA <sup>b</sup>	48 (±2)	0.24 (±0.03)	0.08 (±0.02)	35 (±3)
	3	FRC	NA <sup>b</sup>	45 (±0.6)	0.071 (±0.02)	0.05 (±0.006)	21 (±8)
2	4	P	0.50 (±0.05)	90 (±10)	1.76 (±0.18)	- <sup>c</sup>	93 (±7)
	3	FRP	0.43 (±0.07)	95 (±2)	1.78 (±0.15)	- <sup>c</sup>	79 (±11)
	3	FRC	0.43 (±0.03)	99 (±0.4)	1.59 (±0.03)	- <sup>c</sup>	61 (±12)
3a	1	P	1.64	85	0.65 (±0.03)	0.16 (±0.02)	33 (±10)
	1	FRP <sup>a</sup>	1.75	87	0.76 (±0.02)	0.91 (±0.01)	60 (±5)
	1	FRC <sup>a</sup>	1.85	86	0.20 (±0.007)	0.11 (±0.02)	46 (±2)
3b	3	P	1.54 (±0.17)	90 (±8)	0.88 (±0.12)	0.20 (±0.01)	74 (±5)

<sup>a</sup> Temperature increased to 875 °C to obtain steady flaming. Temperature meets criteria for both stages 3a and 3b.

<sup>b</sup> NA: not applicable for stage 1b.

<sup>c</sup> Below detection limit denoted by dash (-).

SO<sub>3</sub>.

### 3.1. Prediction of incapacitation

Assessment of smoke toxicity was based on toxic product yields, in this work the asphyxiants carbon monoxide, CO, and hydrogen cyanide, HCN, were used to predict incapacitation as a fractional effective dose (FED) according to Eqs. (1) and (2). The yield of CO, in g g<sup>-1</sup>, was calculated on a mass-charge basis according to ISO/TS 19700 and represents the CO concentration resulting from burning a fixed mass of

**Table 4**  
Yields of asphyxiants quantified in fire effluent sampled in different fire stages.

Fire stage	Test	$\phi$	CO Y <sub>m.charge</sub> mg g <sup>-1</sup>	HCN Y UV-vis mg g <sup>-1</sup>	HCN Y HPIC mg g <sup>-1</sup>	H <sub>3</sub> PO <sub>4</sub> Y HPIC mg g <sup>-1</sup>
1b	P	NA <sup>b</sup>	56 (±11)	- <sup>c</sup>	- <sup>c</sup>	- <sup>c</sup>
	FRP	NA <sup>b</sup>	44 (±17)	0.51	0.48	- <sup>c</sup>
	FRC	NA <sup>b</sup>	26 (±13)	- <sup>c</sup>	- <sup>c</sup>	- <sup>c</sup>
2	P	0.50	- <sup>c</sup>	- <sup>c</sup>	- <sup>c</sup>	- <sup>c</sup>
	FRP	0.51	- <sup>c</sup>	- <sup>c</sup>	- <sup>c</sup>	5.36
	FRC	0.46	- <sup>c</sup>	- <sup>c</sup>	- <sup>c</sup>	8.60
3a	P	1.64	158 (±19)	2.63	2.49	- <sup>c</sup>
	FRP <sup>a</sup>	1.75	784 (±10)	6.62	7.50	5.46
	FRC <sup>a</sup>	1.85	97 (±16)	3.04	2.72	14.2
3b	P	1.74	178 (±2)	4.77	5.84	- <sup>c</sup>

<sup>a</sup> Temperature increased to 875 °C to obtain steady flaming. Temperature meets criteria for both stages 3a and 3b.

<sup>b</sup> NA: not applicable for stage 1b.

<sup>c</sup> Below detection limit denoted by dash (-).

sample in a fixed volume under controlled fire conditions. The yield of HCN was calculated likewise based on the cyanide ion quantification. Since the potential for sample losses was greater than the potential for detecting more HCN than was present, the maximum HCN concentration obtained from spectrophotometric or HPIC was used in the estimation, converted to gas concentration, normalized to burning a fixed mass in a fixed volume under controlled fire conditions. As the potential for incapacitation by smoke from stage 3a of FRP and FRC would also correspond to stage 3b, the same data has been shown for both fire conditions. This arises from the need to increase the furnace temperature to 875 °C to ensure steady flaming, so in this case both stages would be tested under identical conditions. Prediction of incapacitation after 5 min exposure to fire effluent, generated from 1 kg timber and distributed in a volume of 50 m<sup>3</sup> for all tested fire stages is shown in Fig. 4 (Data found in SI, S9). As the FRP gave such a high CO yield (784 mg g<sup>-1</sup>) and a high HCN yield (7.5 mg g<sup>-1</sup>) for fire stage 3a/3b, this distorts the comparison resulting in FED of 2.71.

Fig. 4 shows that FRP burning with under-ventilated flaming (fire stages 3a and 3b) is far more incapacitating than the other sample-fire condition combinations; fractional effective doses for samples during well-ventilated flaming (fire stage 2) were calculated to be below 0.01. FRC resulted in - 39% relative decrease in FED compared to Pine (0.49 vs. 0.30) during under-ventilated flaming (-57% by oxidative pyrolysis).

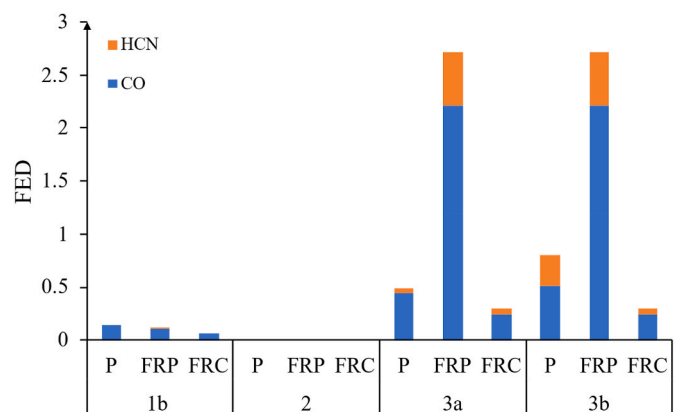


**Fig. 4.** Fractional effective dose (FED) for incapacitation according to ISO 13571 by 5 min exposure to fire effluent generated by combustion of 1 kg timber (Pine (=P), FRP or FRC) distributed in a volume of 50 m<sup>3</sup>.

#### 4. Discussion

**Oxidative Pyrolysis** When the timber samples are exposed to external radiation and undergo oxidative pyrolysis (stage 1b) a remarkable difference in decomposition behaviour of the two fire protecting treatments is observed (Table 3). Yields from both *Pine* and *FRP* were around 0.21–0.24 g g<sup>-1</sup> for CO<sub>2</sub> and 80 mg g<sup>-1</sup> for CO, whereas the yields from *FRC* were significantly lower, at around 0.071 g g<sup>-1</sup> for CO<sub>2</sub> and 50 mg g<sup>-1</sup> for CO. In contrast, *FRC* produced the most smoke, reducing the transmittance in the mixing chamber to 21%. Under these conditions, it appears that the small CO and CO<sub>2</sub> yields, coupled to the larger smoke production suggest that the intumescent coating produces significant quantities of smoke, but effectively protects the underlying timber.

**Well-ventilated flaming** To initiate flaming, the SSTF furnace temperature had to be increased to 875 °C for both treated timbers, as specified in ISO/TS 19700. In comparison, untreated *Pine* showed sustained flaming at 650 °C. Although this may appear to be a significant change of test conditions, it is only the increase in heat flux needed for steady flaming. *Pine* undergoes steady flaming at a furnace temperature of 650 °C. During flaming carbon from the test specimen is converted to a combination of CO<sub>2</sub>, CO, smoke particulates, char, and partially oxidised products such as aldehydes, or hydrocarbons [35]. Based on elemental analysis (C%, Table 2), complete combustion of *Pine* should yield 1.72 g g<sup>-1</sup> CO<sub>2</sub> which is in good agreement with the yield for stage 2 of 1.76 g g<sup>-1</sup> CO<sub>2</sub> (with almost no smoke and complete mass loss). Further, literature reports 4–9 mg g<sup>-1</sup> CO during well-ventilated combustion [36,37], which agrees with the current work (detection limit of sensor 4 ppm). All the timbers tested showed CO yields below detection limits and CO/CO<sub>2</sub> ratios below 0.05 (SI, Fig. S10). Compared to *Pine*, both fire protecting treatments generate more smoke (Fig. 3).

**Under-ventilated flaming** As the fuel-to-air ratio is increased and flaming combustion becomes under-ventilated, the fire behaviour changes. Fig. 2 shows an increase in CO yields with increase in equivalence ratio. CO yields of 160 mg g<sup>-1</sup> are found for *Pine* (stage 3a, Table 3), which is consistent with literature (140 mg g<sup>-1</sup>) [37]. CO/CO<sub>2</sub> ratios as high as 0.24 have been reported [37] for wood, which is again consistent with this study (SI, Fig. S10). In stage 3a, all samples formed around 15 wt% char. However, a surprising difference in combustion products is found: the mass loss yields of CO for *FRP* have increased by +470% compared to *Pine*. This may result from more effective gas-phase quenching of flaming combustion by the penetrative treatment (*FRP*) (favouring CO over CO<sub>2</sub>) or greater char oxidation from the residue of the *FRP* than from the coated sample. From elemental analysis of *FRP*, it is not surprising that both cyanide (N%, Table 2) and phosphorus, reported as phosphoric acid (%P, Table 2), were detected in the fire effluent (Table 4). Even though yields are fairly small, cyanide is potent asphyxiant, contributing to the high FED of 2.71. The finding shows that at least 50% of healthy population would be incapacitated by 5 min exposure to fire effluent developed from under-ventilated flaming of 1 kg of *FRP* with smoke dispersed in a 136 m<sup>3</sup> volume (= 50 × 2.71). In addition, smaller amounts of irritant (H<sub>3</sub>PO<sub>4</sub>) are released, possibly as phosphorus pentoxide (P<sub>2</sub>O<sub>5</sub>), which is volatile at 600 °C, and hydrolyses to 90% orthophosphate in water [38]. In contrast, effluent from *FRC* shows decreased CO yield compared to *Pine* (-31%, Table 3). Despite higher N-content shown in Table 2, cyanide yields for *FRC* were comparable to *Pine*, and the toxic potency of the smoke is lower than for *Pine* itself (FED of 0.30 vs. 0.49, Fig. 4). Thus, in the most toxic under-ventilated flaming for the samples investigated in this study, the coating gives comparable Euroclass ratings for flame spread, and has the lowest smoke toxicity. However, the release of (poly)phosphoric acid is expected due to the presence of APP and from the reactions during intumescence [38]; the toxic potency of phosphoric acid (detected as orthophosphate) is not included in ISO 13571 or ISO 13344 and has not been evaluated in this work.

#### 5. Conclusions

By replication of individual fire stages using the steady state tube furnace and sampling of fire effluent, the smoke toxicity of untreated, surface coated, and fire impregnated plywood was compared. Toxic product yields were determined by real-time sensors and analysis of bubbler solutions by high performance ion chromatography and spectrophotometry. Despite different phosphorus loadings and fire protecting concepts, both treatments showed effective fire protection toward developing fires, with less than 50% mass loss during non-flaming oxidative pyrolysis, and resisted steady flaming. When the fire grows to become under-ventilated, the smoke toxicity of impregnated plywood is demonstrated to be significantly higher in terms of fractional effective dose for incapacitation than for coated timber due to high CO yields (784 mg g<sup>-1</sup> timber, +470%). All samples released CO and HCN while fire protected timbers additionally released H<sub>3</sub>PO<sub>4</sub>. Even though fire protecting treatments target developing fires, and have identical Euroclass flame spread rating (B-s1, d0), the smoke toxicity of phosphorus-based fire protecting treatments must be included in fire risk assessment when selecting products to ensure fire safety in under-ventilated fire stages.

#### CRedit

I. Hansen-Bruhn: Conceptualization, Formal analysis, Investigation, Methodology, Validation, Visualization, Data Curation, Writing - Original Draft, Writing - Review & Editing. T.R. Hull: Conceptualization, Formal analysis, Resources, Project administration, Supervision, Writing - Review & Editing.

#### Declaration of competing interest

The authors declare that they have no known competing financial interests or personal relationships that could have appeared to influence the work reported in this paper.

#### Data availability

The data is contained in the Supplementary Information

#### Acknowledgements

This work was supported by Innovation Fund Denmark [grant no 9065-00233B]. The authors thank Katarina Handlovicova, and Clare Bedford for help with data acquisition.

#### Appendix A. Supplementary data

Supplementary data to this article can be found online at <https://doi.org/10.1016/j.firesaf.2023.103977>.

#### References

- [1] M.H. Ramage, H. Burrige, M. Busse-Wicher, G. Fereday, T. Reynolds, D.U. Shah, O. Scherman, The wood from the trees: the use of timber in construction, *Renew. Sustain. Energy Rev.* 68 (2017) 333–359.
- [2] A.I. Bartlett, R.M. Hadden, L.A. Bisby, A review of factors affecting the burning behaviour of wood for application to tall timber construction, *Fire Technol.* 55 (2019) 1–49.
- [3] B. Östman, D. Brandon, H. Frantzich, Fire safety engineering in timber buildings, *Fire Saf. J.* 91 (2017) 11–20.
- [4] B. Östman, National fire regulations for the use of wood in buildings – worldwide review 2020, *Wood Mater. Sci. Eng.* 17 (1) (2022) 2–5.
- [5] D. Barber, R. Gerard, Summary of the fire protection foundation report-fire safety challenges of tall wood buildings, *Fire Sci. Rev.* 4 (2015) 1–15.
- [6] L.A. Lowden, T.R. Hull, Flammability behaviour of wood and a review of the methods for its reduction, *Fire Sci. Rev.* 2 (2013) 1–19.
- [7] C.M. Popescu, A. Pfriem, Treatments and modification to improve the reaction to fire of wood and wood based products—an overview, *Fire Mater.* 44 (1) (2020) 100–111.



- [8] B. Bahrani, V. Hemmati, A. Zhou, S.L. Quarles, Effects of natural weathering on the fire properties of intumescent fire-retardant coatings, *Fire Mater.* 42 (4) (2018) 413–423.
- [9] T. Mariappan, Fire retardant coatings, *New Tech. Protect. Coat.* 28 (5) (2017).
- [10] W.J. Homan, A.J. Jorissen, Wood modification developments, *Heron* 49 (4) (2004) 360–369.
- [11] B. Östman, A. Voss, A. Hughes, P. Jostein Hovde, O. Grexa, Durability of fire retardant treated wood products at humid and exterior conditions review of literature, *Fire Mater.* 25 (3) (2001) 95–104.
- [12] T. Harada, H. Matsunaga, Y. Kataoka, M. Kiguchi, J. Matsumura, Weatherability and combustibility of fire-retardant-impregnated wood after accelerated weathering tests, *J. Wood Sci.* 55 (2009) 359–366.
- [13] M. Gao, B. Ling, S. Yang, M. Zhao, Flame retardance of wood treated with guanidine compounds characterized by thermal degradation behavior, *J. Anal. Appl. Pyrol.* 73 (1) (2005) 151–156.
- [14] Fire Statistics, United Kingdom, 2022. <https://www.gov.uk/government/statistics/detailed-analysis-of-fires-attended-by-fire-and-rescue-services-england-april-2021-to-march-2022/detailed-analysis-of-fires-attended-by-fire-and-rescue-services-england-april-2021-to-march-2022>. (Accessed 4 February 2023).
- [15] T.R. Hull, R.E. Quinn, I.G. Areri, D.A. Purser, Combustion toxicity of fire retarded EVA, *Polym. Degrad. Stabil.* 77 (2) (2002) 235–242.
- [16] W.M. Pitts, Global equivalence ratio concept and the prediction of carbon monoxide formation in enclosure fires, *Prog. Energy Combust. Sci.* 21 (1995) 197–237.
- [17] T.R. Hull, J.M. Carman, D.A. Purser, Prediction of CO evolution from small-scale polymer fires, *Polym. Int.* 49 (10) (2000) 1259–1265.
- [18] D.A. Purser, Toxic product yields and hazard assessment for fully enclosed design fires, *Polym. Int.* 49 (10) (2000) 1232–1255.
- [19] S.A. Molyneux, A.A. Stec, T.R. Hull, The correlation between carbon monoxide and hydrogen cyanide in fire effluents of flame retarded polymers, *Fire Saf. Sci.* 11 (2014) 389–403.
- [20] A.A. Stec, T.R. Hull, K. Lebek, J.A. Purser, D.A. Purser, The effect of temperature and ventilation condition on the toxic product yields from burning polymers, *Fire Mater.* 32 (1) (2008) 49–60.
- [21] ISO/TS 19706:2011, Guidelines for Assessing the Fire Threat to People, ISO, Geneva.
- [22] Z. Karpovič, R. Šukys, R. Gudelis, Toxicity research of smouldering and flaming pine timber treated with fire retardant solutions, *J. Civ. Eng. Manag.* 18 (4) (2012) 600–608.
- [23] ISO 13571:2012 Life-Threatening Components of Fire - Guidelines for the Estimation of Time to Compromised Tenability in Fires, ISO, Geneva.
- [24] ISO/TS 19700:2016 Controlled Equivalence Ratio Method for the Determination of Hazardous Components of Fire Effluents — Steady-State Tube Furnace, ISO, Geneva.
- [25] D.A. Purser, Fire types and combustion products, in: D.A. Purser, R.L. Maynard, J. Wakefield (Eds.), *Toxicity, Survival and Health Hazards of Combustion Products*, 13–50, Royal Society of Chemistry, Cambridge, 2015.
- [26] D.A. Purser, Toxic combustion product yields as a function of equivalence ratio and flame retardants in under-ventilated fires: bench-large-scale comparisons, *Polymers* 8 (9) (2016) 330.
- [27] A.A. Stec, T.R. Hull, D.A. Purser, J.A. Purser, Fire toxicity assessment: comparison of asphyxiant yields from laboratory and large scale flaming fires, *Fire Saf. Sci.* 11 (2014) 404–418.
- [28] I. Hansen-Bruhn, T.R. Hull, Flammability and burning behaviour of fire protecting timber treatments, *Fire Saf. J.* (2023), 103918.
- [29] T.R. Hull, A.A. Stec, K. Lebek, D. Price, Factors affecting the combustion toxicity of polymeric materials, *Polym. Degrad. Stabil.* 92 (12) (2007) 2239–2246.
- [30] A.A. Stec, T.R. Hull, K. Lebek, Characterisation of the steady state tube furnace (ISO TS 19700) for fire toxicity assessment, *Polym. Degrad. Stabil.* 93 (11) (2008) 2058–2065.
- [31] ISO 19701:2013 Methods for Sampling and Analysis of Fire Effluents, ISO, Geneva.
- [32] I. Hansen-Bruhn, S.T. McKenna, T.R. Hull, Quantification of hydrogen cyanide in fire effluent, *J. Fire Sci.* 41 (5) (2023) 224–237. <https://doi.org/10.1177/07349041231193756>.
- [33] H. Yang, R. Yan, H. Chen, D.H. Lee, C. Zheng, Characteristics of hemicellulose, cellulose and lignin pyrolysis, *Fuel* 86 (12–13) (2007) 1781–1788.
- [34] J. Zhao, W. Xiuwen, J. Hu, Q. Liu, D. Shen, R. Xiao, Thermal degradation of softwood lignin and hardwood lignin by TG-FTIR and Py-GC/MS, *Polym. Degrad. Stabil.* 108 (2014) 133–138.
- [35] S.S. Kropotova, G.V. Kuznetsov, P.A. Strizhak, Identifying products of pyrolysis and combustion of materials at incipient stages of fires, *Fire Saf. J.* 132 (2022), 103643.
- [36] A. Tewarson, Fully developed enclosure fires of wood cribs, in: *Symposium (International) on Combustion*, 20, Elsevier, 1985, pp. 1555–1566, 1.
- [37] P. Blomqvist, T. Hertzberg, H. Tuovinen, K. Arrhenius, L. Rosell, Detailed determination of smoke gas contents using a small-scale controlled equivalence ratio tube furnace method, *Fire Mater.: Int. J.* 31 (8) (2007) 495–521.
- [38] G. Camino, G. Martinasso, L. Costa, R. Gobetto, Thermal degradation of pentaerythritol diphosphate, model compound for fire retardant intumescent systems: Part II – intumescence step, *Polym. Degrad. Stabil.* 28 (1) (1990) 17–38.